Effect of Support on Oxidative Esterification of 2,5-Furandiformaldehyde to Dimethyl Furan-2,5-dicarboxylate

Tingting Ge [1,2], Xiaorui Liu [1], Jie Tang [1,2], Chao Liu [1,*] and Jiahui Huang [1,*]

1   Dalian National Laboratory for Clean Energy, Dalian Institute of Chemical Physics, Chinese Academy of Sciences, Dalian 116023, China; getting@dicp.ac.cn (T.G.); xiaoruil@dicp.ac.cn (X.L.); jaytang@dicp.ac.cn (J.T.)
2   University of Chinese Academy of Sciences, Beijing 100049, China
*   Correspondence: chaoliu@dicp.ac.cn (C.L.); jiahuihuang@dicp.ac.cn (J.H.)

Abstract: One-step oxidative esterification of 2,5-furandiformaldehyde (DFF) derived from biomass to prepare Dimethyl Furan-2,5-dicarboxylate (FDMC) not only simplifies the catalytic process and increases the purity of the product, but also avoids the polymerization of 5-hydroxymethylfurfural (HMF) at high-temperature conditions. Gold supported on a series of acidic oxide, alkaline oxide, and hydrotalcite was prepared using colloidal deposition to explore the effect of support on the catalytic activities. The Au/Mg$_3$Al-HT exhibited the best catalytic activity, with 97.8% selectivity of FDMC at 99.9% conversion of DFF. This catalyst is also suitable for oxidative esterification of benzaldehyde and furfural. X-ray diffraction (XRD), transmission electron microscopy (TEM), X-ray photoelectron spectroscopy (XPS), and CO_2 temperature programmed desorption (CO_2-TPD) were performed to characterize the catalysts. The results indicated that the medium and strong basic sites in the catalysts benefited for the absorption of intermediate agents and facilitated the oxidative esterification of aldehyde groups, while neutral or acidic supports tended to produce an acetal reaction. It is worth noting that basicity on the support surface reduced the electronic state of the Au nanoparticle ($Au^{\delta-}$) and, thus, enhanced the catalytic selectivity of oxidative esterification. This finding demonstrated that the support plays a crucial role in oxidative esterification.

Keywords: oxidative esterification; Au nanoparticles; support effects

1. Introduction

Biomass energy is the fourth largest source of energy after oil, coal, and natural gas and has an important role in the international energy transformation. The conversion of non-edible biomass raw materials into utilizable chemicals through catalysis is one important way to achieve the sustainable development of resources in an environmentally friendly manner. 2,5-furanodicarboxylic acid (FDCA) is the most promising biomass molecule for polymerization with ethylene glycol to obtain Polyethylene 2,5-furandicarboxylate (PEF) [1], which can be used as an alternative material to polyethylene terephthalate (PET). However, due to the poor solubility of FDCA in most industrial solvents, the conversion process from FDCA to PEF is tricky [2], and the separation of FDCA is tough using conventional purification methods. Additionally, in this reaction, 5-hydroxymethyl furfural (HMF) is used as the substrate molecule and hydroxyl group oxidation is the rate-limiting step, which makes the process difficult [3]. Different from FDCA, Dimethyl Furan-2,5-dicarboxylate (FDMC) has good solubility in organic solvents. FDMC has a low boiling point, which makes FDMC easy to purify with vacuum distillation, as well.

Currently, heterogeneous catalysts for the oxidative esterification of HMF to FDMC mainly contain the noble metals Au and Pd and the non-noble metal Co. In the process of oxidative esterification of HMF to FDMC, alkaline additives are indispensable for creating an alkaline environment. Li et al. [4] used PdCoBi/C catalysts to convert HMF to FDMC with a yield of 96% under mild conditions. Abel et al. [5] achieved 100% selectivity of

FDMC using Co/Ru bimetallic to catalyze HMF. Au nanocatalysts have been widely used for oxidative esterification because of their unique stability [6], especially in HMF oxidative esterification to FDMC. Supported gold catalysts have high activity in the oxidation of aldehyde groups [7]; the HMF turnover frequency of Au ranged from 2 to 5 s^{-1}. In the past few decades, there have been many reports about the preparation of FDMC on Au nanoparticles under alkaline conditions. Christensen et al. [8] used an Au/TiO_2 catalyst in the oxidative esterification of HMF, and a 98% FDMC yield was obtained. Au nanoparticles sPSB [9] could convert HMF to FDMC with a 98% yield. Waclawik et al. [10] constructed an $Au/\gamma\text{-}Al_2O_3$ catalyst with a three-dimensional irregular stack structure and achieved a more than 90% yield of FDMC at low reaction temperature.

However, the presence of excessive alkaline additives (such as NaOH, K_2CO_3, and KOH) not only leads to an increase in salt by-products and a rise in separation costs but also destroys the active sites on the catalyst surface. Conversely, in the absence of alkaline additives, Au is easily deactivated due to the effect of carboxylic acid intermediates [11]. Therefore, alkaline supports are often used as a potential alternative to alkaline additives. Song et al. [12] used an organic base group-grafted silica aerogel-supported Au to catalyze oxidative esterification of furfural, and the yield of methyl furoate was above 98%. Ferraz [13] used an Au/MgO catalyst in the oxidative esterification of furfural, achieving a methyl furoate yield of 95%. Kim et al. [14] used a series of gold catalysts supported by hydroxyapatite and achieved an 89.3% yield of FDMC from HMF oxidative esterification in the absence of additional alkali. Recently, Li et al. [15] found that the nano-gold catalyst supported by Mg-Al hydrotalcite showed good activity for DFF oxidative esterification, with a 96% yield of FDMC.

In the process of alcohol oxidation catalyzed by heterogeneous catalysts, the adsorption of substrates on the active sites usually determines the reaction mechanism and product selectivity [16]. According to oxidative esterification with a gold-based catalyst, the negatively charged $Au^{\delta-}$ nanoparticles are more likely to activate HMF and methanol [17]. Huo et al. [18] constructed an Au-ZrO_x interface and obtained a 99.4% yield of FDCA by modulating the crystalline phase structure of ZrO_2, proving that the electron transfer between Au and ZrO_2 is conducive to promoting the adsorption of O_2. Transition metal oxide modified Au/TiO_2 catalyzed the oxidative esterification of HMF; 100% HMF conversion and more than 90% FDCA yield could be obtained, showing that the electron-rich $Au^{\delta-}$ on the catalyst surface enhanced the interaction between reactants and catalysts [16]. Au base alloy catalysts can also achieve an FDMC yield of 85%, imparted by the synergistic effect between different metal components [19].

Although there have been many reports on the preparation of FDMC using the oxidation of HMF, there are still several problems in the conversion of HMF to FDMC. (1) The HMF usually contains impurities and humins, resulting in poor-quality PEF. (2) PEF showing yellow is usually caused by the decomposition of FDCA at high temperatures during the polymerization of FDCA with ethylene glycol. In order to solve this problem, Jia et al. proposed replacing HMF with 2,5-furandiformaldehyde (DFF) for oxidative esterification to prepare FDMC [3]. Compared with the traditional catalytic route, using DFF can not only solve the problem of low purity of the product but also avoid the oxidation of the hydroxyl group to enhance catalytic activity. Therefore, the reaction process is more controllable, and the cost of separation is much lower.

In this paper, we used DFF as the raw material and Mg-Al hydrotalcite-supported gold as the catalyst to obtain FDMC via a one-step oxidative esterification process. We investigated the effects of support on the acid–base property and the electron state of Au on catalytic activity, and provide a reference for the catalyst design of FDMC production from DFF. The oxidative esterification of DFF to prepare FDMC is helpful for simplifying the production process of furan esters from fructose; compared with HMF as raw material, the product quality can be improved to some extent.

2. Results and Discussion

2.1. Catalysts Characterization

The XRD pattern of several basic oxides and hydrotalcite-supported Au catalysts is characterized in Figure 1. The diffraction peaks in all the samples agree well with the PDF cards of the supports. Of note, the XRD diffraction angle of Mg_2Al-HT shifted to a smaller angle after the Mg-Al molar ratio was reduced to 2:1, indicating that the layer spacing of the hydrotalcite structure became larger with increased aluminum content. Extremely weak diffraction peaks appeared for gold (111) in Au/Mg_3Al-HT, showing that the size of Au nanoparticles is small. TEM images display the mean size distribution of gold nanoparticles on the surface of different catalysts in Figure 2. The mean size of gold nanoparticles was uniformly distributed at about 5–6 nm, which confirmed that the four types of supports hardly affect the size of Au nanoparticles. The Au content was tested with ICP-OES in the supported catalyst, and the content of Au was 0.39 wt%.
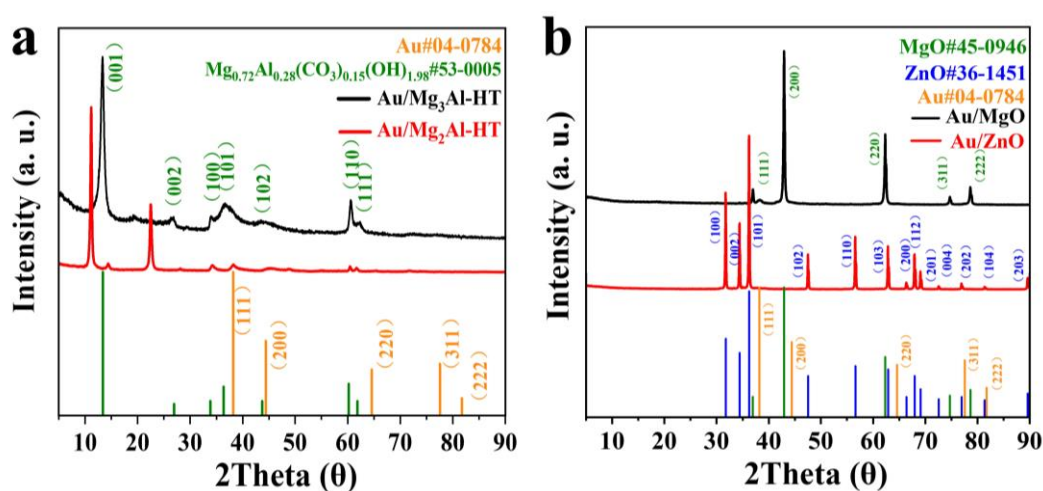
Figure 1. (**a**) XRD pattern of Au/Mg_3Al-HT and Au/Mg_2Al-HT, (**b**) Au/MgO and Au/ZnO.
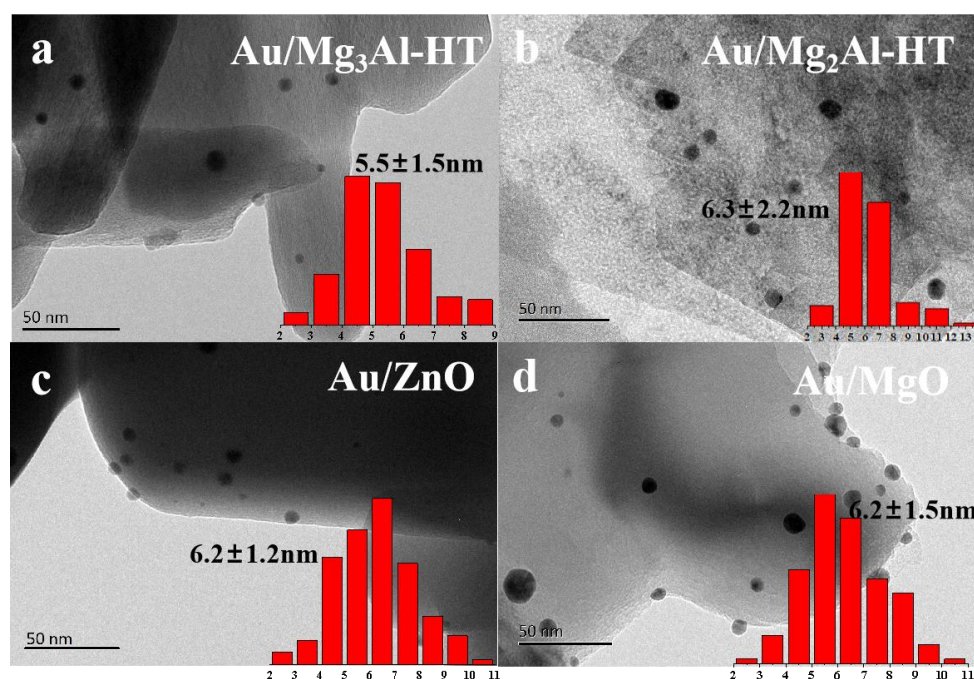
Figure 2. TEM images of (**a**) Au/Mg_3Al-HT, (**b**) Au/Mg_2Al-HT, (**c**) Au/ZnO, (**d**) Au/MgO. Inset shows the particle size distribution of Au nanoparticles.

Heterogeneous gold catalysts used for oxidative reactions often exhibit higher reactivity in the presence of a base [20]. The catalysts with abundant surface hydroxyl groups also showed higher catalytic activity in the aldehyde oxidative [21]. In order to determine appropriate support, the catalytic performance of a series of oxide and hydrotalcite-supported Au catalysts was tested in oxidative esterification of DFF. The reaction was conducted at 140 °C and 2 MPa air for 8 h. The possible conversion paths for oxidative esterification of DFF in methanol are listed in Scheme 1. According to the catalytic performance, the catalysts Au/SiO$_2$, Au/TiO$_2$, Au/CeO$_2$, Au/ZrO$_2$, and Au/Al$_2$O$_3$ showed 80% selectivity of bis(dimethoxymethyl)furan (BDM) and 20% selectivity of 5-(dimethoxymethyl) furan-2-carbaldehyde (FFDM) at the complete conversion of DFF (Figure 3). La$_2$O$_3$ and ZnO-supported Au catalysts had a high yield of FDMC (74.6% for Au/La$_2$O$_3$, 83.8% for Au/ZnO) under 99% conversion of DFF, and the by-product was methyl 5-(dimethoxymethyl) furan-2-carboxylate (DMME). Au/Mg$_3$Al exhibited the best catalytic activity, with 97.8% selectivity of FDMC at 99% conversion. It is worth noting that when the Mg-Al ratio was 2:1, the selectivity of FDMC and the carbon balance of the reaction decreased significantly. The amount of reactants lost was 49.5%, and only 42.4% of 5-(methoxycarbonyl) furan-2-carboxylic acid (MECA) was collected. Similar to Au/Mg$_2$Al-HT, significant carbon loss (34.3%) was also found on the Au/MgO catalyst. Due to the high carbon loss, Au/MgO had a 99% selectivity for FDMC, but the yield of the target product was only 65.7%. Therefore, these activity experiments directly reflected the influence of supports on product selectivity. In general, those catalysts with base sites (Au/Mg$_3$Al-HT, Au/Mg$_2$Al-HT, Au/ZnO, Au/MgO, and Au/La$_2$O$_3$) allowed obtaining oxidative esterification products, while catalysts with acid sites could only obtain acetals after the reaction [22]. According to the literature [2], basic supports could encourage the hemiacetal to be converted to ester, but acidic supports prefer to convert hemiacetals to acetals, which is a reversible process. In oxidative esterification of DFF, the presence of base sites is crucial for promoting DFF oxidative esterification. Additionally, different basicities of the supports affect the carbon balance of the reaction and the reaction intermediates of esterification. When Au/Mg$_3$Al-HT, Au/Mg$_2$Al-HT, and Au/MgO were used as catalysts, we detected the presence of magnesium salts in the solution after the reaction, indicating that the loss of magnesium in the supports could hinder the further esterification of the intermediate products (carboxylic acids). The reaction intermediates reacted with magnesium ions to form salt, which further led to the carbon loss.
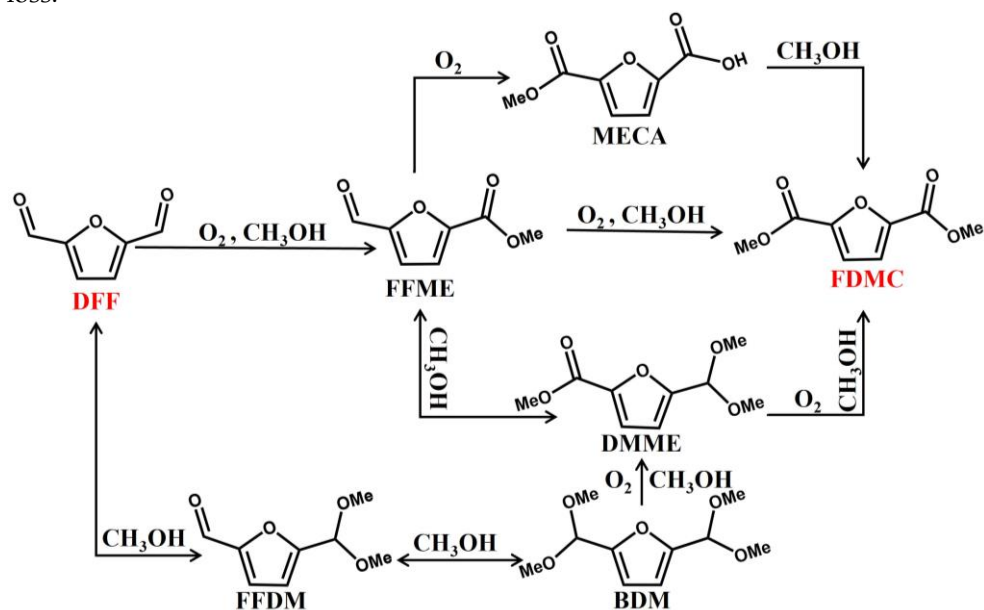
Scheme 1. Possible reaction paths of oxidative esterification of DFF in methanol. (DFF: 2,5-furandiformaldehyde is the substrate; FDMC: Dimethyl Furan-2,5-dicarboxylate is the target product.)
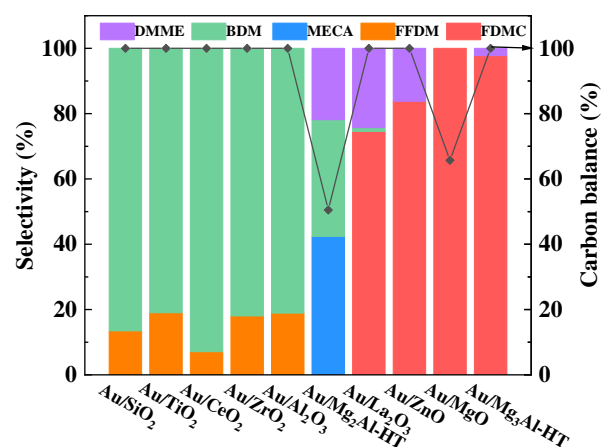
Figure 3. Oxidative esterification of DFF over Au catalysts with different supports.

In order to characterize the strength of alkalinity on different supports, CO_2-TPD analysis was carried out on the basic supported Au catalysts. In Figure 4a, Au/Mg$_3$Al-HT shows the maximum desorption quantity of CO_2 between 350 and 600 °C, and Au/La$_2$O$_3$ shows an obvious CO_2 desorption signal between 600 and 800 °C. For Au/Mg$_2$Al-HT, Au/MgO, and Au/ZnO, the temperature between 250 and 600 °C shows very weak signals. Corresponding to the different CO_2 desorption temperatures, the basic sites on the catalyst surface can be divided into weak basic sites (<250 °C), medium basic sites (250–400 °C), strong basic sites (400–600 °C), and super basic sites (>600 °C) [22]. It is commonly acknowledged that the weakly basic site is provided by the -OH group on the surface of catalysts for the formation of hydrogen bonds, the medium basic site is provided by M-O pairs, and the strong basic site is from lattice oxygen [23]. Furthermore, considering the possible presence of acidic sites on the catalysts' surface, we performed NH$_3$-TPD to test these five catalysts. In Figure 4b, Au/Mg$_3$Al-HT also shows the strongest NH$_3$ desorption signal between 400 and 600 °C. For Au/Mg$_2$Al-HT, Au/MgO, Au/ZnO, and Au/La$_2$O$_3$, they all show similar weak NH$_3$ signals.
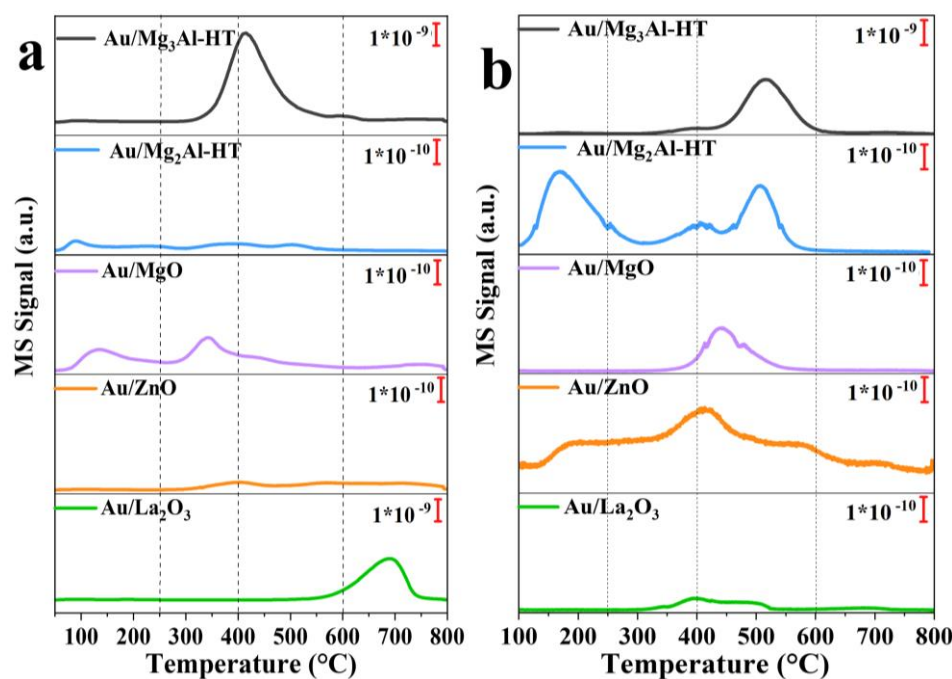
Figure 4. (**a**) CO_2-TPD; (**b**) NH$_3$-TPD desorption profile obtained for Au/Mg$_3$Al-HT, Au/Mg$_2$Al-HT, Au/ZnO, Au/MgO, and Au/La$_2$O$_3$.

According to the catalytic results, the Mg_3-Al_1 hydrotalcite catalyst exhibits significantly higher CO_2 and NH_3 adsorption capacity. It is generally believed that the acidic site on the catalyst surface is conducive to the adsorption and polarization of aldehyde groups of DFF [24], further promoting the nucleophilic attack of methanol to form hemiacetal intermediates. In the presence of alkaline sites, hemiacetal intermediates are more inclined to bind with Au on the catalyst surface to promote the formation of esters [13]. Au/La_2O_3 showed a strong CO_2 desorption signal above 600 °C but with a very weak NH_3 adsorption capacity; the yield of FDMC is only 74.6%. Au/Mg_2Al-HT, Au/MgO, and Au/ZnO had similar CO_2 and NH_3 desorption patterns, but these catalysts exhibited different catalytic activities. Au/Mg_2Al-HT produced a large amount of acetal products (57.6%). Au/MgO led to a significant amount of carbon loss (34.3%). In contrast, Au/ZnO could obtain a FDMC yield of more than 80% (Figure 3). Based on these results, the number of medium and strong alkaline sites and appropriate acidic sites had an effect on catalyst activity in oxidative esterification.

In order to further determine the correlation between the electron states of Au on the catalyst surface and the catalytic activity of the catalyst, XPS characterization was carried out on gold catalysts with those five alkaline supports, and the results are shown in Figure 5. It is noteworthy that on the surface of several alkaline supports, the electron binding energy of the Au $4f_{7/2}$ shifted to a lower binding energy than that of the metallic Au (84.0 eV). Au on Au/Mg_3Al-HT had the lowest Au $4f_{7/2}$ electron binding energy (83.32 eV), followed by 83.46 eV for Au/ZnO, 83.63 eV for Au/La_2O_3, 83.96 eV for Au/Mg_2Al-HT, and 83.97 eV for Au/MgO, indicating that higher electron density is favorable for DFF oxidative esterification. The stronger electron transfer between Au and the carrier makes Au $^{\delta-}$ more active for the activation of C-H bonds in DFF [25], benefiting the formation of the ester. Therefore, Au/Mg_3Al-HT with the appropriate density of base sites [26] and rich electronics on an active surface are more advantageous for substrate adsorption activation and facilitate obtaining a higher FDMC yield.
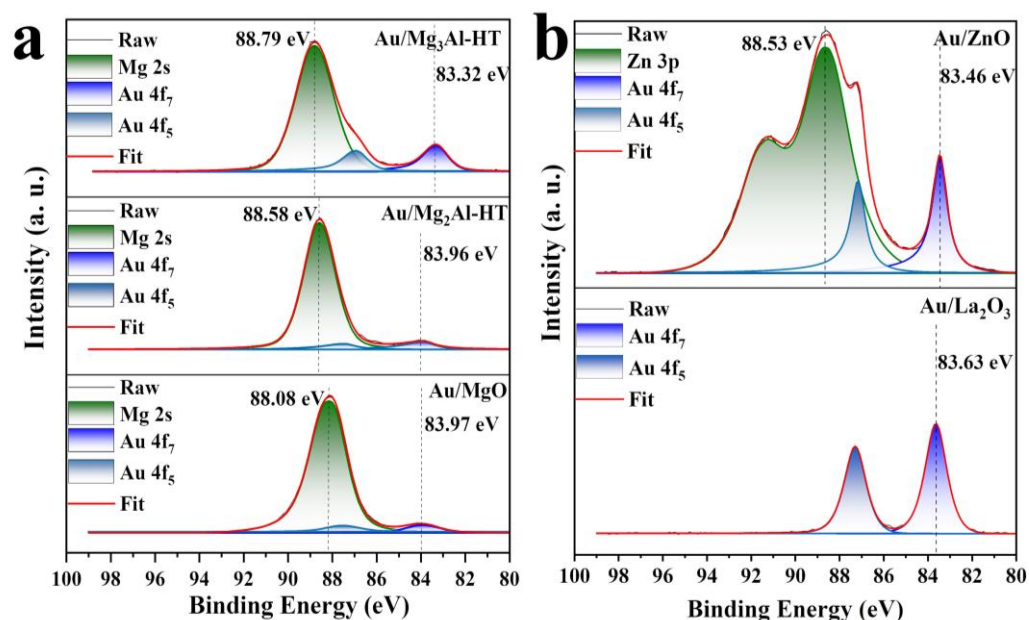
Figure 5. XPS spectra of (**a**) Au/Mg_3Al-HT, Au/Mg_2Al-HT, and Au/MgO; (**b**) Au/ZnO and Au/La_2O_3.

2.2. Effect of the Calcination Temperature of the Catalyst

Here, the effect of calcination temperature on the yield of FDMC is discussed. Different calcination temperatures usually affect the exposure of active sites on the surface of catalysts and the dispersion of active metal components [27]. Au/Mg_3Al-HT catalysts were treated for 2 h at 200 °C, 300 °C, and 500 °C, respectively. The TEM image in Figure 6a,b shows

residual PVP on the surface of the Au/Mg$_3$Al-HT-RT catalyst without heat treatment. The active sites on the catalyst surface were covered by PVP, which led to lower activity of the Au/Mg$_3$Al-HT-RT catalyst [28]. In Figure 6c,d, after calcination at 500 °C, the surfactant on the catalyst was completely removed, but the size of gold nanoparticles increased to 9.1 nm. In Figure 6, after calcination at 500 °C, hydrotalcite was transformed into Mg$_x$Al$_y$O$_z$. As shown in Figure 7a, the relationship between the yield of FDMC and the calcination temperature of catalyst presents a volcanic curve. The catalyst without heat treatment had low activity (92.9% of DFF conversion, 27.8% selectivity for FDMC, and 65.1% for methyl 5-formylfuran-2-carboxylate (FFME)). After calcinating at 200 °C, 69.7% FDMC could be obtained with 20.4% DMME. When the calcination temperature was 500 °C, the reaction results (83.4% of the conversion, 25.8% selectivity for FDMC, and 35.4% for FFME) were close to the results of Au/Mg$_3$Al-HT without heat treatment. After calcining at 300 °C, the catalyst could achieve more than 99.9% conversion and 97.8% yield of FDMC. These results demonstrate that proper calcination temperature can expose active sites of Au nanoparticles and inhibit the acetal reaction.
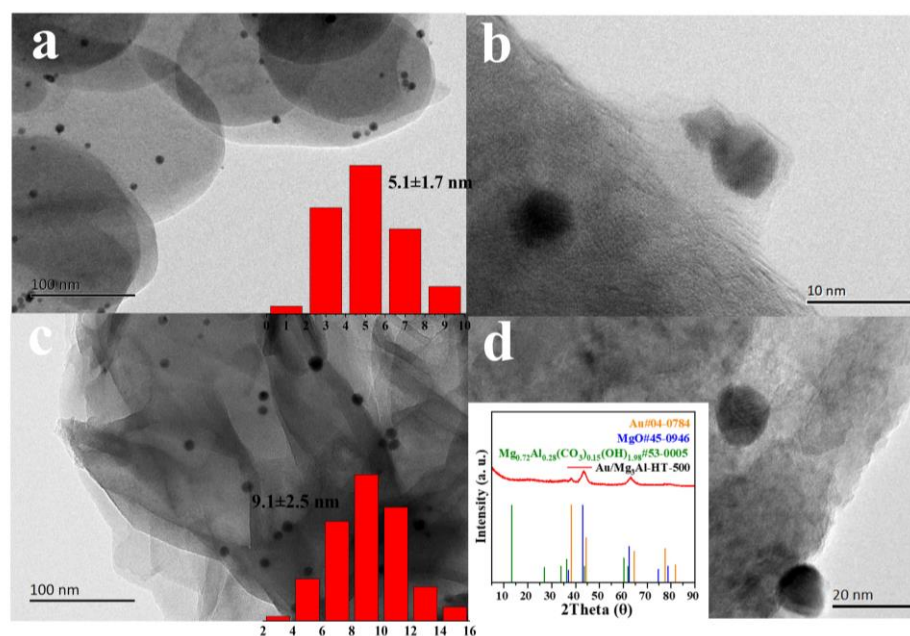
Figure 6. TEM images of (**a**,**b**) Au/Mg$_3$Al-HT-RT, (**c**,**d**) Au/Mg$_3$Al-HT-500. Inset shows the particle size distribution of Au nanoparticles and XRD pattern of Au/Mg$_3$Al-HT-500.
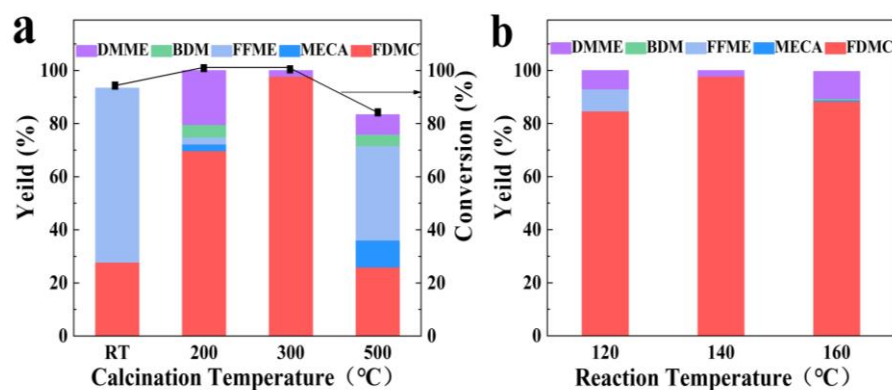
Figure 7. (**a**) Oxidative esterification of DFF on Au/Mg$_3$Al-HT catalyst with different calcination temperatures, (**b**) Oxidative esterification of DFF at different reaction temperatures using Au/Mg$_3$Al-HT catalyst.

2.3. Effect of Reaction Temperature

The confirmation of the catalyst with the best catalytic activity prompted us to screen for the best reaction conditions. In oxidative reactions, the reaction temperature usually has a significant impact on the conversion rate of the substrate. An Au/Mg$_3$Al-HT catalyst was used to catalyze the oxidative esterification of DFF with methanol at 120 °C, 140 °C, and 160 °C, respectively. In Figure 7b, under 160 °C, the high reaction temperature led to an increase in acetals (88.4% for FDMC, 10.3% for DMME with trace MECA and BDM). When the reaction temperature decreased to 120 °C, the FDMC yield was 84.7%, with 8.3% FFME and 7.0% DMME. At 140 °C, the highest FDMC yield was 97.8%, and only 2.2% DMME was obtained. These results indicate that an over-high reaction temperature is conducive to improved activity of acidic sites, leading to an increase in acetal reaction. On the other hand, due to the limitation of the reaction energy barrier, a decreasing reaction temperature would lead to an increase in monoester products [29].

We plotted the reaction time curve of DFF oxidative esterification on Au/Mg$_3$Al-HT catalysts by collecting the reaction products at different reaction stages (Figure 8). After 1 h of reaction, the yield of FDMC was 31.1%, with 95.7% conversion of DFF. DFF can be completely transformed by prolonging the reaction time. The yield of FDMC showed a slight decrease after 3 h, and then FDMC gradually increased with the extension of time. During the reaction, the yield of detectable by-products was always maintained below 20%. After 8 h of reaction, DMME was the only by-product, with a yield of 2.22%. Based on the reaction time curve, we proposed a possible reaction mechanism in the oxidative esterification of DFF under Au/Mg$_3$Al-HT catalysis. DFF was easily adsorbed and activated on the electron-rich surface of the catalyst, and 5-formylfuran-2-carboxylic acid (FFCA) was obtained at first. After that, FFCA was catalyzed to form FFME through oxidative esterification. The further oxidative esterification of FFME is easier than that of the unilateral aldehyde group of DFF, which makes FFME easy to convert further into FDMC.
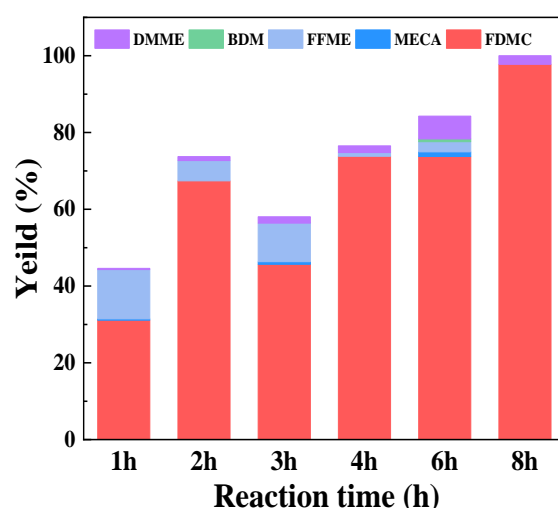
Figure 8. Oxidative esterification of DFF using Au/Mg$_3$Al-HT catalyst with different times.

2.4. Catalytic Performance of Au/Mg$_3$Al-HT on Different Substrates

We investigated the catalytic ability of an Au/Mg$_3$Al-HT catalyst for the oxidative esterification of different aldehyde substrates, including benzaldehyde and furfural. As shown in Table 1 (entry 1, 2), the catalyst shows high activity for the reactants with single aldehyde groups, as well. The yield of corresponding esters could achieve more than 97%. When different kinds of fatty alcohols were used as solvents for oxidative esterification of DFF (Table 1, entry 3–6), it was evident that the conversion of DFF and the yield of esterification products steadily declined as the carbon atoms of the solvent increased. The larger steric hindrance of alcohols impeded the esterification process. At the same time, the

products of the solvent's self-oxidative polymerization gradually increased. The higher activity of hydrogen atoms in hydroxyl and smaller steric hindrance makes methanol easier for esterification.

Table 1. Oxidative esterification of different substrates using Au/Mg$_3$Al-HT catalyst.

Entry	Substrate	Solvent	Conv.	(di)Ester	Monoester	Monoacetal	Monoester-Monoacetal	(di)Acetal
entry 1	FF [1]	methanol	100.00	97.23	/	/	/	2.77
entry 2	BzH [2]	methanol	100.00	99.01	/	/	/	0.99
entry 3	DFF	methanol	100.00	97.78	/	/	/	2.22
entry 4	DFF	ethanol	100.00	54.61	12.89	6.47	24.45	1.57
entry 5	DFF	n-butanol	94.02	6.65	3.76	82.59	6.99	/
entry 6	DFF	1-pentanol	59.24	/	2.60	34.56	62.84	/

[1] Furfural. [2] Benzyl alcohol. Reaction condition: Substrate: Au = 200: 1; Solvent: 15 mL; Atmosphere: air, 2 MPa; Reaction time: 8 h; Reaction temperature: 140 °C.

2.5. Stability of Au/Mg$_3$Al-HT Catalyst

To evaluate the catalyst's stability, the catalytic activity of Au/Mg$_3$Al-HT-Used was tested under the same reaction conditions. The results showed that the activity of the Au/Mg$_3$Al-HT catalyst decreased significantly, with 99.9% conversion and 73.7% selectivity. To explore the reasons for catalyst deactivation, the Au loading of the catalyst after the reaction was tested with ICP-OES; the metal load remained essentially constant at 0.3786 wt%, indicating that there was no significant loss of the Au active component. The XRD pattern showed that the structure of the catalyst did not significantly change for the used catalyst. In Figure 9a, the diffraction peak intensity of the hydrotalcite (001) surface decreased. Combined with the ICP-OES data, the content of magnesium in the solution after the reaction was 2.6113 mg/L; that is, the magnesium loss of Au/Mg$_3$Al-HT was 0.4766% after one use. The loss of magnesium during the reaction results in the deformation of the surface structure of the support. At the same time, the peak intensity of the (111) and (311) planes of Au increased after the reaction, proving that the size of Au nanoparticles slightly increased [30] (Figure 9a). The TEM image also confirmed that Au nanoparticles on the catalyst surface increased from 5.5 nm to 6.8 nm after the first cycle (Figure 9b). XPS characterization showed that the binding energy of Au4f$_{7/2}$ of the used catalyst was still at 83.31 eV (Figure 9d). These characterization results show that the loss of the support basic site and the reduction in active sites might be the primary factors in the deactivation of catalysts.
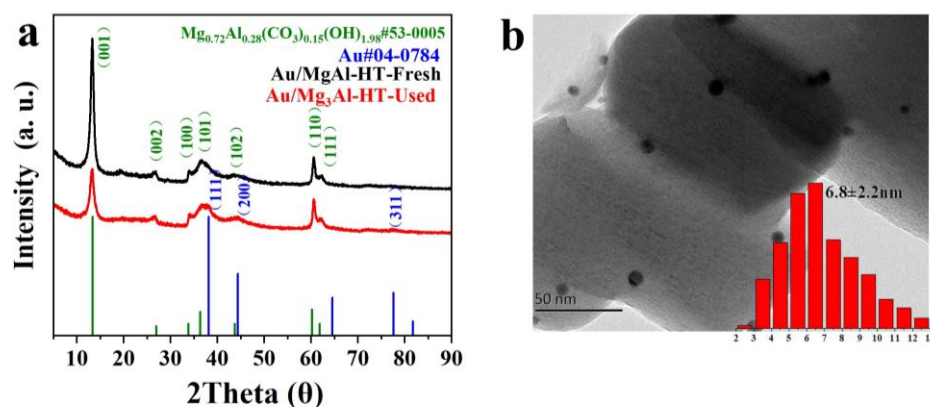
Figure 9. *Cont.*
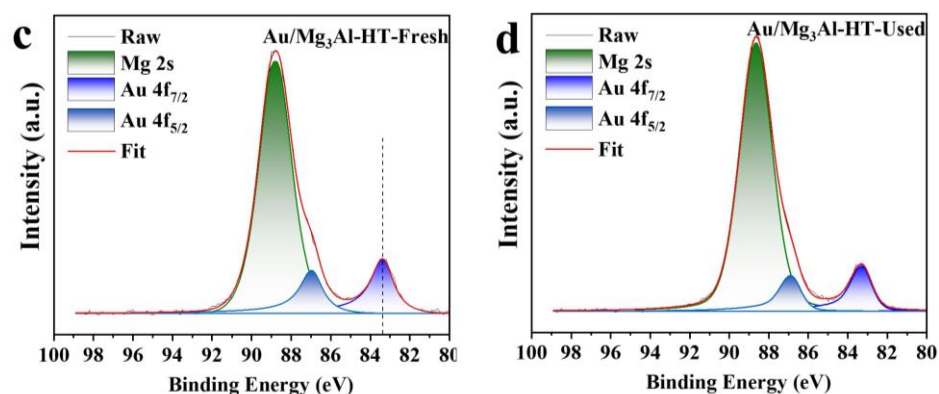
Figure 9. (**a**) XRD pattern of Au/Mg$_3$Al-HT-Fresh and Au/Mg$_3$Al-HT-Used, (**b**) TEM image of Au/Mg$_3$Al-HT-Used; (**c**) XPS Spectra of Au/Mg$_3$Al-HT-Fresh and (**d**) Au/Mg$_3$Al-HT-Used.

3. Materials and Methods

3.1. Materials

Tetrachloroauric(III) acid (HAuCl$_4$·4H$_2$O, >99.99% metals basis, Sinopharm Chemical Reagent Co., Ltd., Shanghai, China), Polyvinylpyrrolidone (average M.W. 8000, K16-18, ACROS ORCANICS, Geel, Belgium), Sodium borohydride (NaBH$_4$, >98%, Sinopharm Chemical Reagent Co., Ltd., Shanghai, China), Aluminium oxide (Al$_2$O$_3$, >99.99% metals basis, 40 nm, MACKLIN, Shanghai, China), Hydrotalcite (Al$_2$Mg$_6$·CO$_3$·16(OH)·4(H$_2$O), >98%, HEOWNS, Tianjin, China), Magnesium oxide (MgO, AR, Kermel, Tianjin, China), Zinc oxide (ZnO, AR, Kermel, Tianjin, China), Lanthanum oxide (La$_2$O$_3$, AR, Kermel, Tianjin, China), Zirconium dioxide (ZrO$_2$, >99.0%, Sinopharm Chemical Reagent Co., Ltd., Shanghai, China), Cerium oxide (CeO$_2$, AR, Kermel, Tianjin, China), Titanium(IV) oxide (Aeroxide P25, ACROS ORCANICS, Geel, Belgium), Magnesium nitrate hexahydrate (Mg(NO$_3$)$_2$·6H$_2$O, AR, Kermel, Tianjin, China), Aluminum nitrate nonahydrate (Al(NO$_3$)$_3$·9H$_2$O, AR, Sinopharm Chemical Reagent Co., Ltd., Shanghai, China), Urea (CH$_4$N$_2$O, AR, Sinopharm Chemical Reagent Co., Ltd., Shanghai, China), Methyl alcohol (CH$_3$OH, AR, Sinopharm Chemical Reagent Co., Ltd., Shanghai, China), Ethanol (CH$_3$CH$_2$OH, AR, Sinopharm Chemical Reagent Co., Ltd., Shanghai, China).

3.2. Preparation of the Catalyst

Preparation of Mg$_2$Al-HT support: Magnesium aluminum hydrotalcite (Mg$_2$Al-HT) was prepared with the precipitation deposition method, referring to the literature [31]. Magnesium nitrate hexahydrate (20 mmol) and aluminum nitrate hexahydrate (10 mmol) were dissolved in 200 mL of deionized water. Then, the pH of the solution was adjusted to 12 by dropwise adding ammonium hydroxide and stirring at room temperature for 20 min. The reaction stood at room temperature for 1 h, and then the precipitation was centrifuged and washed with water three times. The precipitation was dispersed in 70 mL of deionized water and transferred to a polytetrafluoroethylene reactor at 140 °C for 72 h. After the reaction, the product was centrifuged and dried. The product was calcined at 200 °C for 2 h to remove the water molecules of the hydrotalcite.

Preparation of Au/Mg$_3$Al-HT catalyst: Supported gold catalysts were prepared using the colloidal deposition method. First, 11 mg of chlorauric acid tetrahydrate was dissolved in 45 mL of anhydrous ethanol, and 70 mg polyvinylpyrrolidone (Mw = 8000) was added to the above solution. After 30 min, an alcohol solution of sodium borohydride (2.1 mg sodium borohydride dissolved in 2.5 mL ethanol) was quickly introduced into the reaction solution. The solution color quickly changed from light yellow to wine red, and the reaction continued for 1 h at room temperature. Au nanoparticles were diluted by the addition of twice the volume of ethanol. Next, 529 mg of Mg$_3$Al-HT was added to the Au solution. The precipitation was centrifugated and dried in a vacuum for 12 h. After calcination at 300 °C for 2 h, the Au/Mg$_3$Al-HT catalyst was obtained. Other supported Au catalysts with different oxides were prepared following the same method. The theoretical loading

of the metal for all catalysts was 1 wt% (the actual metal load was 0.394 wt% according to ICP-OES).

3.3. Catalytic Evaluation

One-step oxidative esterification of DFF to FDMC was carried out in a stainless-steel high-pressure reactor. First, 33.2 mg DFF, 15 mL methanol, 26.2 mg cat., and 100 μL dodecane (internal standard substance) were added into the reactor, and 2 MPa of air was filled after sealing the reactor. In 30 min, the reactor temperature rose to 140 °C, the magnetic stirring speed was set at 1000 rmp, and the reaction time was 8 h. After the reaction, the reactor was quickly transferred to cold water to cool down. The reaction products were analyzed with GC-MS (GC, Agilent 7890 A, Agilent Technologies, Santa Clara, CA, USA), equipped with HP-5 (30 m, 0.32 mm).

4. Conclusions

A series of oxide and hydrotalcite-supported gold catalysts were prepared for catalyzing DFF oxidative esterification to FDMC. The catalytic performance demonstrated that basic supports made the catalysts more active for oxidative esterification. When using Mg_3Al-HT as the catalyst support, the FDMC yield achieved 97.8%. The Au/Mg_3Al-HT also exhibited outstanding catalytic performance to oxidative esterification of other aldehyde substrates. According to CO_2-TPD and XPS characterization, the concentration of alkaline sites on the catalyst surface and the electronic structure of Au both had an important impact on the catalytic activity. It was found that the loss of alkaline sites caused by the fall off of magnesium from the support during the reaction is a major factor of catalyst deactivation. Therefore, there are still problems with the stability of the support to be solved. The preparation of high-purity FDMC from DFF provides an idea for the improvement of the process of producing biomass-derived polyester plastics.

Author Contributions: Conceptualization, T.G.; methodology, T.G. and X.L.; software, X.L.; investigation, T.G.; resources, J.T.; data curation, T.G.; writing—original draft preparation, T.G. and X.L.; writing—review and editing, C.L. and J.H.; visualization, X.L.; supervision, C.L. and J.H.; project administration, C.L. and J.H.; funding acquisition, J.H. All authors have read and agreed to the published version of the manuscript.

Funding: This work received financial support from the Projects of International Cooperation and Exchanges NSFC (No. 21961142006).

Data Availability Statement: The data presented in this study are available on request from the corresponding author. The data are not publicly available due to privacy or ethical restrictions.

Conflicts of Interest: The authors declare no conflict of interest.

References

1. Burgess, S.K.; Leisen, J.E.; Kraftschik, B.E.; Mubarak, C.R.; Kriegel, R.M.; Koros, W.J. Chain Mobility, Thermal, and Mechanical Properties of Poly (ethylene furanoate) Compared to Poly (ethylene terephthalate). *Macromolecules* **2014**, *47*, 1383–1391. [CrossRef]
2. Casanova, O.; Iborra, S.; Corma, A. Biomass into chemicals: One pot-base free oxidative esterification of 5-hydroxymethyl-2-furfural into 2,5-dimethylfuroate with gold on nanoparticulated ceria. *J. Catal.* **2009**, *265*, 109–116. [CrossRef]
3. Jia, W.; Chen, J.; Yu, X.; Zhao, X.; Feng, Y.; Zuo, M.; Li, Z.; Yang, S.; Sun, Y.; Tang, X.; et al. Toward an integrated conversion of fructose for two-step production of 2,5-furandicarboxylic acid or furan-2,5-dimethylcarboxylate with air as oxidant. *Chem. Eng. J.* **2022**, *450*, 138172. [CrossRef]
4. Li, F.; Li, X.-L.; Li, C.; Shi, J.; Fu, Y. Aerobic oxidative esterification of 5-hydroxymethylfurfural to dimethyl furan-2,5-dicarboxylate by using homogeneous and heterogeneous PdCoBi/C catalysts under atmospheric oxygen. *Green Chem.* **2018**, *20*, 3050–3058. [CrossRef]
5. Salazar, A.; Hünemörder, P.; Rabeah, J.; Quade, A.; Jagadeesh, R.V.; Mejia, E. Synergetic Bimetallic Oxidative Esterification of 5-Hydroxymethylfurfural under Mild Conditions. *ACS Sustain. Chem. Eng.* **2019**, *7*, 12061–12068. [CrossRef]
6. Takei, T.; Akita, T.; Nakamura, I.; Fujitani, T.; Haruta, M. Heterogeneous Catalysis by Gold. *Adv. Catal.* **2012**, *55*, 1–126. [CrossRef]
7. Davis, S.E.; Houk, L.R.; Tamargo, E.C.; Datye, A.K.; Davis, R.J. Oxidation of 5-hydroxymethylfurfural over supported Pt, Pd and Au catalysts. *Catal. Today* **2011**, *160*, 55–60. [CrossRef]

8. Taarning, E.; Nielsen, I.S.; Egeblad, K.; Madsen, R.; Christensen, C.H. Chemicals from Renewables: Aerobic Oxidation of Furfural and Hydroxymethylfurfural over Gold Catalysts. *ChemSusChem* **2008**, *1*, 75–78. [CrossRef]

9. Buonerba, A.; Impemba, S.; Litta, A.D.; Capacchione, C.; Milione, S.; Grassi, A. Aerobic Oxidation and Oxidative Esterification of 5-Hydroxymethylfurfural by Gold Nanoparticles Supported on Nanoporous Polymer Host Matrix. *ChemSusChem* **2018**, *11*, 3139–3149. [CrossRef]

10. Weerathunga, H.; Sarina, S.; Zhu, H.Y.; Waclawik, E.R. Oxidative Esterification of 5-Hydroxymethylfurfural into Dimethyl 2,5-Furandicarboxylate Using Gamma Alumina-Supported Gold Nanoparticles. *ACS Omega* **2021**, *6*, 4740–4748. [CrossRef]

11. Dimitratos, N.; Villa, A.; Wang, D.; Porta, F.; Su, D.; Prati, L. Pd and Pt catalysts modified by alloying with Au in the selective oxidation of alcohols. *J. Catal.* **2006**, *244*, 113–121. [CrossRef]

12. Song, F.; Cen, S.; Wan, C.; Wang, L. Nano-Au Anchored in Organic Base Group-Grafted Silica Aerogel: A Durable and Robust Catalysts for Green Oxidative Esterification of Furfural. *ChemCatChem* **2022**, *14*, e202200704. [CrossRef]

13. Ferraz, C.P.; Braga, A.H.; Ghazzal, M.N.; Zieliński, M.; Pietrowski, M.; Itabaiana, I.; Dumeignil, F.; Rossi, L.M.; Wojcieszak, R. Efficient Oxidative Esterification of Furfural Using Au Nanoparticles Supported on Group 2 Alkaline Earth Metal Oxides. *Catalysts* **2020**, *10*, 430. [CrossRef]

14. Mishra, D.K.; Cho, J.K.; Yi, Y.; Lee, H.J.; Kim, Y.J. Hydroxyapatite supported gold nanocatalyst for base-free oxidative esterification of 5-hydroxymethyl-2-furfural to 2,5-furan dimethylcarboxylate with air as oxidant. *J. Ind. Eng. Chem.* **2019**, *70*, 338–345. [CrossRef]

15. Guo, X.; Si, Y.; Huang, Y.; Zhang, J.; Lyu, X.; Cheng, Y.; Li, X. Base-Free Oxidative Esterification of HMF Using Mg–Al Hydrotalcite-Supported Gold Catalyst. *Ind. Eng. Chem. Res.* **2023**, *62*, 16309–16318. [CrossRef]

16. Yang, W.; Fu, M.; Yang, C.; Zhang, Y.; Shen, C. Au^-–O_v–Ti^{3+}: Active site of MO-Au/TiO$_2$ catalysts for the aerobic oxidation of 5-hydroxymethylfurfural. *Green Energy Environ.* **2023**, *8*, 785–797. [CrossRef]

17. Menegazzo, F.; Fantinel, T.; Signoretto, M.; Pinna, F.; Manzoli, M. On the process for furfural and HMF oxidative esterification over Au/ZrO$_2$. *J. Catal.* **2014**, *319*, 61–70. [CrossRef]

18. Zhang, Y.; Cao, Y.; Yan, C.; Liu, W.; Chen, Y.; Guan, W.; Wang, F.; Liu, Y.; Huo, P. Rationally designed Au-ZrO$_x$ interaction for boosting 5-hydroxymethylfurfural oxidation. *Chem. Eng. J.* **2023**, *459*, 141644. [CrossRef]

19. Campisi, S.; Bellomi, S.; Chinchilla, L.E.; Prati, L.; Villa, A. Base-free Oxidative Esterification of HMF over AuPd/nNiO-TiO$_2$. When Alloying Effects and Metal-Support Interactions Converge in Producing Effective and Stable Catalysts. *ChemCatChem* **2022**, *14*, e202200494. [CrossRef]

20. Ide, M.S.; Davis, R.J. The Important Role of Hydroxyl on Oxidation Catalysis by Gold Nanoparticles. *Acc. Chem. Res.* **2014**, *47*, 825–833. [CrossRef]

21. Zhu, Z.; Gao, X.; Wang, X.; Yin, M.; Wang, Q.; Ren, W.; Wang, B.; Lü, H.; Liao, W. Rational construction of metal–base synergetic sites on Au/Mg-beta catalyst for selective aerobic oxidation of 5-hydroxymethylfurfural. *J. Energy Chem.* **2021**, *62*, 599–609. [CrossRef]

22. Ren, J.; Mebrahtu, C.; Palkovits, R. Ni-based catalysts supported on Mg–Al hydrotalcites with different morphologies for CO$_2$ methanation: Exploring the effect of metal–support interaction. *Catal. Sci. Technol.* **2020**, *10*, 1902–1913. [CrossRef]

23. Dębek, R.; Radlik, M.; Motak, M.; Galvez, M.E.; Turek, W.; Da Costa, P.; Grzybek, T. Ni-containing Ce-promoted hydrotalcite derived materials as catalysts for methane reforming with carbon dioxide at low temperature—On the effect of basicity. *Catal. Today* **2015**, *257*, 59–65. [CrossRef]

24. Liu, H.; Jia, W.; Yu, X.; Tang, X.; Zeng, X.; Sun, Y.; Lei, T.; Fang, H.; Li, T.; Lin, L. Vitamin C-Assisted Synthesized Mn–Co Oxides with Improved Oxygen Vacancy Concentration: Boosting Lattice Oxygen Activity for the Air-Oxidation of 5-(Hydroxymethyl)furfural. *ACS Catal.* **2021**, *11*, 7828–7844. [CrossRef]

25. Liao, Y.; Yan, H.; Zhou, J.; Yue, Y.; Sun, Y.; Peng, T.; Yuan, X.; Zhou, X.; Liu, Y.; Feng, X.; et al. Interfacial $Au^{\delta-}$-O_V-Zr^{3+} structure promoted C H bond activation for oxidative esterification of methacrolein to Methyl methacrylate. *Chem. Eng. J.* **2023**, *454*, 140322. [CrossRef]

26. Wan, Q.; Wang, X.; Zhao, B.; Zhao, G.; Zhao, G.; Gao, E.; Gong, Y.; Yu, H.; Wang, X.; Liu, D.; et al. Influence of calcination temperature on the cooperative catalysis of base sites and gold nanoparticles on hydrotalcite-supported gold materials for the base-free oxidative esterification of 1,3-propanediol with methanol to methyl 3-hydroxypropionate. *React. Kinet. Mech. Catal.* **2021**, *134*, 109–125. [CrossRef]

27. Sankar, M.; He, Q.; Engel, R.V.; Sainna, M.A.; Logsdail, A.J.; Roldan, A.; Willock, D.J.; Agarwal, N.; Kiely, C.J.; Hutchings, G.J. Role of the Support in Gold-Containing Nanoparticles as Heterogeneous Catalysts. *Chem. Rev.* **2020**, *120*, 3890–3938. [CrossRef]

28. Monti, E.; Ventimiglia, A.; Soto, C.A.G.; Martelli, F.; Rodríguez-Aguado, E.; Cecilia, J.A.; Maireles-Torres, P.; Ospitali, F.; Tabanelli, T.; Albonetti, S.; et al. Oxidative condensation/esterification of furfural with ethanol using preformed Au colloidal nanoparticles. Impact of stabilizer and heat treatment protocols on catalytic activity and stability. *Mol. Catal.* **2022**, *528*, 112438. [CrossRef]

29. Wojcieszak, R.; Ferraz, C.; Sha, J.; Houda, S.; Rossi, L.; Paul, S. Advances in Base-Free Oxidation of Bio-Based Compounds on Supported Gold Catalysts. *Catalysts* **2017**, *7*, 352. [CrossRef]

30. Wei, Y.; Zhang, Y.; Chen, Y.; Wang, F.; Cao, Y.; Guan, W.; Li, X. Crystal Faces-Tailored Oxygen Vacancy in Au/CeO$_2$ Catalysts for Efficient Oxidation of HMF to FDCA. *ChemSusChem* **2021**, *15*, e202101983. [CrossRef]

31. Zhao, D.; Sheng, G.; Hu, J.; Chen, C.; Wang, X. The adsorption of Pb (II) on Mg$_2$Al layered double hydroxide. *Chem. Eng. J.* **2011**, *171*, 167–174. [CrossRef]